Inorg. Chem. **2007**, *46*, 10491–10500

Structural and Thermodiffractometric Analysis of Coordination Polymers. Part I: Tin Derivatives of the Bim ligand [Bim = Bis(1-imidazolyl)methane])

Norberto Masciocchi,[†] Claudio Pettinari,*[,‡] Enrica Alberti,[†] Riccardo Pettinari,[‡] Corrado Di Nicola,[‡] Alessandro Figini Albisetti,[§] and Angelo Sironi*[,§]

Dipartimento di Scienze Chimiche e Ambientali, Università dell'Insubria, via Valleggio 11, 22100 Como, Italy, Dipartimento Scienze Chimiche, Università di Camerino, via S. Agostino 1, 62032 Camerino, Italy, and Dipartimento di Chimica Strutturale e Stereochimica Inorganica, Università di Milano, via Venezian 21, 20133 Milano, Italy

Received August 1, 2007

New polynuclear coordination species containing the ditopic bis(1-imidazolyl)methane (Bim) ligand have been prepared as microcrystalline powders and structurally characterized by ab initio X-ray powder diffraction methods. $[Bim(Me_2SnCl_2)]_n$ (**1**), $[Bim(^nBu_2SnCl_2)]_n$ (**3**), $[Bim(Ph_2SnCl_2)]_n$ (**4**), $[Bim(MeSnCl_3)]_n$ (**5**), and $[Bim(PhSnCl_3)]_n$ (**6**) all contain 1D chains with octahedral tin atoms with trans N–Sn–N linkages (but **4**, which displays a cis N–Sn–N linkage). Their thermodiffractometric analysis allowed the estimation of the linear thermal expansion coefficients and strain tensors derived there from. The potential-energy surface of the free Bim ligand (as defined by two torsional degrees of freedom about the two N–CH_2 bonds), eventually controlling the length of the repeating unit (polymer elongation), has been estimated using molecular mechanics and correlated with experimental observations.

Introduction

Incorporation of inorganic elements into polymers offers the prospect of properties that combine the advantages of ceramics, semiconductors, metals, or optical materials with the characteristics of classical organic polymers. It is now commonly accepted that design and synthesis of novel coordination polymers with unusual and tailorable structures are fundamental steps to discover and fabricate various technologically useful materials.[1−4] Most of the literature species have been constructed from organic ligands and metal ions by spontaneous self-assembly. Recently, much effort has been devoted to the design and construction of new supramolecular frameworks using metal clusters or metal−organic secondary building units as building blocks and polydentate organic ligands as linkers.[5,6] Such assembly has resulted in a host of intriguing structural topologies and an extensive application in material science.[7]

There has been a renewed interest in organotin polymers too. Such polymers are used mainly for the controlled release of bioactive compounds while simultaneously minimizing environmental hazards. Studies involving the antiviral activities of organotin polymers, derived from the antiviral agent acyclovir and the antibiotic ciprofloxacin, have been reported by Roner and co-workers.[8]

In our recent work we studied linear, two- and three-dimensional metal organic frameworks containing *anionic* angular linkers (pyrazolates, imidazolates, and pyrimidinolates) and transition-metal centers, aiming at construction of extended solids not containing counterions in the crystal lattice, favoring formation of nanoporous materials. As a first

* To whom correspondence should be addressed. E-mail: angelo.sironi@unimi.it.
† Università dell'Insubria.
‡ Università di Camerino.
§ Università di Milano.

(1) Hagrman, P. J.; Hagrman, D.; Zubieta, J. *Angew. Chem., Int. Ed. Engl.* **1999**, *38*, 2638−2684.
(2) Kitagawa, S.; Kitaura, R.; Noro, S. *Angew. Chem., Int. Ed.* **2004**, *43*, 2334−2375.
(3) Herrmann, W. A.; Goossen, L. J.; Spiegler, M. *Organometallics* **1998**, *17* (11), 2162−2168.
(4) Sanchez, C.; Lebeau, B.; Chaput, F.; Boilot, J. P. *Adv. Mater.* **2003**, *15*, 1969−1994.
(5) Eddaoudi, M.; Moler, D. B.; Li, H.; Chen, B.; Reineke, T. M.; O'Keeffe, M.; Yaghi, O. M. *Acc. Chem. Res.* **2001**, *34*, 319−330.
(6) Yaghi, O. M.; Li, H.; Davis, C.; Richardson, D.; Groy, T. *Acc. Chem. Res.* **1998**, *31*, 474−484.
(7) See, for example: Rowsell, J. L. C.; Millward, A. R.; Park, K. S.; Yaghi, O. M. *J. Am. Chem. Soc.* **2004**, *124*, 5666−5667.
(8) Shahi, K.; Roner, M. R.; Carraher, C. E., Jr.; Barot, G. *Polym. Mater. Sci. Eng.* **2006**, *94*, 466−468.

10.1021/ic701530c CCC: $37.00
Published on Web 11/15/2007

Chart 1

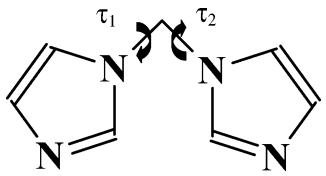

step toward the preparation of extended materials containing slightly larger angular ligands, we have now resorted to bis-(imidazolyl)methane (Bim), which is a versatile, flexible, bridging bidentate ligand bearing an alkyl spacer between two imidazole unities, first prepared by Shutze in 1959 (see Chart 1).[9] Some reports describe Bim as a carbonic anhydrase activator,[10] and its interaction with the zinc enzyme carbonic anhydrase has been investigated also.[11] This ligand has been also employed as a precursor of ionic liquid systems.[12] A novel macrocyclic anion receptor has been synthesized using Bim that has proved to be an effective receptor for F^- ions. Modification of this system would allow the development of a new class of calix containing many positively charged moieties that would be suitable for anion recognition by ionic hydrogen-bonding interactions and as precursors for N-heterocyclic carbenes for application in metal coordination chemistry.[13]

Despite the potentialities of this ligand, few metal complexes have been isolated and characterized. Cui and coworkers reported eight new complexes with 1D, 2D, or 3D framework structures by self-assembly of two structurally related flexible bis(imidazole) ligands with Ag^I, Cu^{II}, Zn^{II}, and Cd^{II} salts.[14] The same authors also reported the crystal structure of two other complex Cu^{II} polymers.[15,16] Two lithium-based organic−inorganic hybrid materials based on bis(imidazolyl) moieties with interesting topochemical properties have been very recently described. In both cases, lithium exhibits unusually high binding affinity toward the nitrogen atoms of bisimidazole moiety. Interestingly it has been reported that the properties of the polymers could easily be fine tuned by varying the nature of the substituents inherent to the bis(imidazole) moiety.[17]

Here we describe the interaction of Bim with the Lewis-acidic metal centers SnR_nX_{4-n} (n = 2, 3, or 4, X = Cl or Br, R = Me, Et, Ph, Bu^n, or X), affording several one-dimensional, polycrystalline polymers which have been structurally characterized from laboratory X-ray powder diffraction data only using the ab initio technique developed in the last years in our laboratories. We further characterized these species by thermodiffractometry (aiming at understanding molecular flexibility in the crystals in the lattice through analysis of thermal expansion coefficients and thermal strain tensors), solid-state CP-MAS NMR studies, and modeling of the torsional energy associated with the C−N rotations of the free ligand.

This paper, in which only organometallic Sn(IV) species are reported, is followed by another contribution in which harder Lewis bases (Zn(II) and Cd(II) ions) are employed, showing a large variety of molecular/crystal topologies from 0D to 3D ones. It is worth noting that some of the structural results reported therein will be anticipated in the final portion of this contribution while commenting on the stereochemical preferences of the Bim ligand.

Experimental Section

Materials and Methods. All chemicals and reagents were of reagent-grade quality and used as received without further purification. All solvents were distilled prior to use. THF and light petroleum (310−333 K) were dried by refluxing over freshly cut sodium. Dichloromethane was freshly distilled from CaH_2. Other solvents were dried and purified by standard procedures. The samples were dried in vacuo to constant weight (293 K, 0.1 Torr). Elemental analyses were carried out in house with a Fisons Instruments 1108 CHNSO-elemental analyzer. IR spectra from 4000 to 150 cm^{-1} were recorded with a Perkin-Elmer System 2000 FT-IR instrument. ^1H, $^{13}C\{^1H\}$, and ^{119}Sn NMR solution spectra were recorded on a VXR-300 Varian spectrometer (300 MHz for ^1H 75 MHz for ^{13}C and 117.9 MHz for ^{119}Sn). Referencing is relative to TMS (^1H and ^{13}C) and Me_4Sn (^{119}Sn). NMR samples were prepared by dissolving a suitable amount of compound in 0.5 mL of solvent.

Syntheses. Bim. The ligand Bim, the synthesis of which has already been reported,[18−20] has been prepared following the procedure described in ref 20 and recrystallized from hot chloroform. Mp 165−168 °C. Anal. Calcd for $C_7H_8N_4$: C, 56.74; H, 5.44; N, 37.81. Found: C, 56.83; H, 5.65; N, 37.46. IR (Nujol, cm^{-1}): 3126w, 3111w, 1708w, 1688w, 1658w, 1602w, 1557w, 1503w, 380w, 282w, 279w, 247m, 227w. ^1H NMR (DMSO-d_6, 293K): δ 6.19 (s, 2H, CH_{2Bim}), 6.88 (pd, 2H, CH_{Bim}), 7.38 (pt, 2H, CH_{Bim}), 7.91 (pd, 2H, CH_{Bim}). ^1H NMR (acetone, 293 K): δ 6.31 (s, 2H, CH_{2Bim}), 6.99 (m, 2H, CH_{Bim}), 7.32 (pd, 2H, CH_{Bim}), 7.98 (pd, 2H, CH_{Bim}). ^1H NMR ($CDCl_3$, 293 K): δ 6.01 (s, 2H, CH_{2Bim}), 6.99 (m, 2H, CH_{Bim}), 7.12 (pd, 2H, CH_{Bim}), 7.66 (pd, 2H, CH_{Bim}). ^1H NMR (CD_3OD, 293 K): δ 6.27 (s, 2H, CH_{2Bim}), 7.01 (pd, 2H, CH_{Bim}), 7.33 (pd, 2H, CH_{Bim}), 7.95 (pd, 2H, CH_{Bim}).

$[Bim(Me_2SnCl_2)]_n$ (1). A diethyl ether:ethanol 1:1 solution (20 mL) containing Me_2SnCl_2 (0.219 g, 1.0 mmol) and bis(imidazol-1-yl)methane (Bim) (0.148 g, 1.0 mmol) was stirred for 48 h under N_2 at room temperature. The resulting colorless precipitate was isolated by filtration and dried in vacuum. The obtained residue was washed with 5 mL of diethyl ether and recrystallized from

(9) Schutze, W.; Schubert, H. *J. Physiol.* **1959**, *8*, 306−313.
(10) Supuran, C. T.; Balaban, A. T.; Cabildo, P.; Claramunt, R. M.; Lavandera, J. L.; Elguero, J. *Biol. Pharm. Bull.* **1993**, *16*, 1236−9.
(11) Supuran, C. T.; Claramunt, R. M.; Lavandera, J. L.; Elguero, J. *Biol. Pharm. Bull.* **1996**, 19, 1417−1422.
(12) Jin, C.-M.; Twamley, B.; Shreeve, J. M. *Organometallics* **2005**, *24*, 3020−3023.
(13) Chellappan, K.; Singh, N. J.; Hwang, I.-C.; Lee, J. W.; Kim, K. S. *Angew. Chem., Int. Ed.* **2005**, *44*, 2899−2903.
(14) Cui, G.-H.; Li, J.-R.; Tian, J.-L.; Bu, X.-H.; Batten, S. R. *Cryst. Growth Des.* **2005**, *5*, 1775−1780.
(15) Catena-poly[[bis(isothiocyanato-κN)copper(II)]-bis(μ-1,1′-methylenedi-1*H*-imidazole-κN^3:$\kappa N^{3'}$): Cui, G.-H.; Dong G.-Y.; Ribas, J. *Acta Crystallogr.* **2006**, *E62*, m523−m525.
(16) μ-1,1′-Methylenedi-1*H*-imidazole-κ^2N^3:$N^{3'}$-bis[aqua(pyridine-2,6-dicarboxylato)copper(II)] tetrahydrate: Dong, G.-Y.; Cui, G.-H.; Wang, S.-C. *Acta Crystallogr.* **2006**, *E62*, m606−m607.
(17) Hwang, I. C.; Chandran, R. P.; Singh, N. J.; Khandelwal, M.; Thangadurai, T. D.; Lee, J. W.; Chang, J. A.; Kim, K. S. *Inorg. Chem.* **2006**, *45*, 8062−8069.
(18) Lorenzotti, A.; Cecchi, P.; Pettinari, C.; Leonesi, D.; Bonati, F. *Gazz. Chim. Ital.* **1991**, *121*, 89.
(19) Pettinari, C.; Marchetti, F.; Lorenzotti, A.; Gioia Lobbia, G.; Leonesi, D.; Cingolani, A. *Gazz. Chim. Ital.* **1994**, *124*, 51−55.
(20) Pettinari, C.; Santini, C.; Leonesi, D.; Cecchi, P. *Polyhedron* **1994**, *13*, 1553−1562.

ethanol and shown to be compound **1** (0.331 g, 0.90 mmol, yield 90%). Mp 238 °C (dec). Anal. Calcd for $C_9H_{14}Cl_2N_4Sn$: C, 29.39; H, 3.84; N, 15.23. Found: C, 29.63; H, 3.98; N, 15.19. IR (Nujol, cm^{-1}): 3127w, 3115w, 1593w, 1514s, 1505s υ(C⋯C, C⋯N), 568s υ(Sn−Cl), 382w, 365w, 240s υ(Sn−Cl). ^{1}H NMR (acetone, 293 K): δ 1.23 (s, 6H, CH_{3Sn}, $^2J(^{119}Sn-^1H)$ 90 Hz, $^2J(^{117}Sn-^1H)$ 86 Hz), 6.41 (s, 2H, CH_{2Bim}), 7.04 (pd, 2H, CH_{Bim}), 7.43 (pd, 2H, CH_{Bim}), 8.04 (s, 2H, CH_{Bim}). ^{1}H NMR (DMSO-d_6, 293 K): δ 1.02 (s, 6H, CH_{3Sn}, $^2J(^{119}Sn-^1H)$ 115 Hz, $^2J(^{117}Sn-^1H)$ 110 Hz), 6.24 (s, 2H, CH_{2Bim}), 6.96 (pd, 2H, CH_{Bim}), 7.43 (pd, 2H, CH_{Bim}), 8.04 (s, 2H, CH_{Bim}). ^{1}H NMR (CD_3OD, 293 K): δ 1.03 (s, 6H, CH_{3Sn}, $^2J(^{119}Sn-^1H)$ 139 Hz, $^2J(^{117}Sn-^1H)$ 135 Hz), 6.38 (s, 2H, CH_{2Bim}), 7.17 (d, 2H, CH_{Bim}), 7.46 (d, 2H, CH_{Bim}), 8.25 (s, 2H, CH_{Bim}), Λ_m (DMSO, 10^{-3} M): 17.5 Ω^{-1} cm^2 mol^{-1}. Λ_m (acetone, 10^{-3} M): 1.0 Ω^{-1} cm^2 mol^{-1}.

[Bim(Et_2SnCl_2)] (2). Compound **2** (0.341 g, 0.86 mmol, yield 86%) was prepared following a procedure similar to that reported for **1** using Bim and Et_2SnCl_2. Mp 253−255 °C (dec). Anal. Calcd for $C_{11}H_{18}Cl_2N_4Sn$: C, 33.37; H, 4.58; N, 14.15. Found: C, 33.58; H, 4.45; N, 14.22. IR (Nujol, cm^{-1}): 3120sh, 3106w, 1505s υ(C⋯C, C⋯N), 533m, 388br, 360br, 231br υ(Sn−Cl). ^{1}H NMR (CD_3OD, 293 K): δ 1.38 (t, 6H, CH_{3Sn}), 1.68 (q, 4H, CH_{2Sn}), 6.36 (s, 2H, CH_{2Bim}), 7.13 (d, 2H, CH_{Bim}), 7.42 (d, 2H, CH_{Bim}), 8.18 (s, 2H, CH_{Bim}).

[Bim($^nBu_2SnCl_2$)]$_n$ (3). Compound **3** (0.200 g, 0.43 mmol, yield 43%) was prepared following a procedure similar to that reported for **1** using Bim and $^nBu_2SnCl_2$. Mp 180−182 °C (dec). Anal. Calcd for $C_{15}H_{26}Cl_2N_4Sn$: C, 39.86; H, 5.80; N, 12.40. Found: C, 39.51; H, 5.96; N, 12.31. IR (Nujol, cm^{-1}): 3143sh, 3120w, 3103w, 1558m, 1520 υ(C⋯C, C⋯N), 623 υ(Sn−Cl), 400m, 278m, 240sbr υ(Sn−Cl). ^{1}H NMR (acetone-d_6, 293 K): δ 0.90 (t, 6H, CH_{3Sn}), 1.41 (m, 4H, CH_{2Sn}), 1.80 (br, 8H, CH_{2Sn}), 6.42 (s, 2H, CH_{2Bim}), 6.98 (pd, 2H, CH_{Bim}), 7.40 (pd, 2H, CH_{Bim}), 8.12 (s, 2H, CH_{Bim}). ^{1}H NMR (CD_3OD, 293 K): δ 0.91 (t, 6H, CH_{3Sn}), 1.43 (m, 4H, CH_{2Sn}), 1.7 (m, 8H, CH_{2Sn}), 6.38 (s, 2H, CH_{2Bim}), 7.16 (pd, 2H, CH_{Bim}), 7.44 (pd, 2H, CH_{Bim}), 8.22 (s, 2H, CH_{Bim}). Λ_m (DMSO, 10^{-3} M): 21.7 Ω^{-1} cm^2 mol^{-1}. Λ_m (acetone, 10^{-3} M): 0.3 Ω^{-1} cm^2 mol^{-1}.

[Bim(Ph_2SnCl_2)]$_n$ (4). Compound **4** (0.395 g, 0.80 mmol, yield 80%) was prepared following a procedure similar to that reported for **1** using Bim and Ph_2SnCl_2. Mp 242−245 °C. Anal. Calcd for $C_{19}H_{18}Cl_2N_4Sn$: C, 46.39; H, 3.69; N, 11.39. Found: C, 46.51; H, 3.76; N, 11.21. IR (Nujol, cm^{-1}): 3110w, 3092w, 1580w, 1560w, 1520m υ(C⋯C, C⋯N), 458s, 399w, 377w, 353w, 291s υ_{as}(Sn−C), 253s, 229s υ_s(Sn−C) + υ_{as}(Sn−Cl). ^{1}H NMR (DMSO-d_6, 293 K): δ 6.20 (s, 2H, CH_{2Bim}), 6.90 (pd, 2H, CH_{Bim}), 7.34 (m, 6H, Sn−C_6H_5, $^2J(^{119}Sn-^1H)$ = 92 Hz), 7.40 (pd, 2H, CH_{Bim}), 7.70, 7.91 (d, 4H, Sn−C_6H_5), 8.02 (s, 2H, CH_{Bim}). ^{1}H NMR (acetone-d_6, 293 K): δ 6.21 (s, 2H, CH_{2Bim}), 7.02 (pd, 2H, CH_{Bim}), 7.35 (m, 6H, Sn−C_6H_5), 7.40 (pd, 2H, CH_{Bim}), 7.72, 7.90 (d, 4H, Sn−C_6H_5), 8.00 (s, 2H, CH_{Bim}). Λ_m (DMSO, 10^{-3} M): 9.3 Ω^{-1} cm^2 mol^{-1}. Λ_m (acetone, 10^{-3} M): 0.5 Ω^{-1} cm^2 mol^{-1}.

[Bim($MeSnCl_3$)]$_n$ (5). Compound **5** (0.354 g, 0.91 mmol, yield 91%) was prepared following a procedure similar to that reported for **1** using (Bim) and $MeSnCl_3$. Mp 270 °C (dec). Anal. Calcd for $C_8H_{11}Cl_3N_4Sn$: C, 24.75; H, 2.86; N, 14.43. Found: C, 24.55; H, 2.94; N, 14.22. IR (Nujol, cm^{-1}): 3126w, 3121w, 3080w, 1519w, 1500br υ(C⋯C, C⋯N), 543m υ_{as}(Sn−C), 381m, 326m, 299s, 284s, 272s, 210m, 200m υ(Sn−Cl). ^{1}H NMR (DMSO-d_6, 293 K): δ 0.99 (sbr, 3H, CH_{3Sn}, $^2J(^{119}Sn-^1H)$ = 129 Hz, $^2J(^{117}Sn-^1H)$ = 124 Hz), 6.29 (sbr, 2H, CH_{2Bim}), 7.02 (br, 2H, CH_{Bim}), 7.47 (br, 2H, CH_{Bim}), 8.20 (br, 2H, CH_{Bim}). ^{119}Sn NMR (DMSO-d_6, 293 K): −451.0, −454, −468. Λ_m (DMSO, 10^{-3} M): 41.4 Ω^{-1} cm^2 mol^{-1}. Λ_m (acetone, 10^{-3} M): 0.7 Ω^{-1} cm^2 mol^{-1}.

[Bim($PhSnCl_3$)]$_n$ (6). Compound **6** (0.395 g, 0.87 mmol, yield 87%) was prepared following a procedure similar to that reported for **1** using Bim and $PhSnCl_3$. Mp 310 °C (dec). Anal. Calcd for $C_{13}H_{13}Cl_3N_4Sn$: C, 34.67; H, 2.91; N, 12.44. Found: C, 34.76; H, 2.85; N, 12.29. IR (Nujol, cm^{-1}): 3120w, 1570m, 1538m υ(C⋯C, C⋯N), 560br, 448m, 363m, 309s, 300s υ(Sn−Cl) 290s, 272sh υ(Sn−C), 250m, 220m. ^{1}H NMR (DMSO-d_6, 293 K): δ 6.48 (s, 2H, CH_{2Bim}), 7.32 (m, 6H, Sn−C_6H_5), 7.37 (s, 2H, CH_{Bim}), 7.74 (pd, 2H, CH_{Bim}), 7.89 (pd, 4H, Sn−C_6H_5, $^2J(Sn-^1H)$ = 109), 8.78 (pd, 2H, CH_{Bim}). ^{13}C NMR (DMSO-d_6, 293 K): δ 56.7 (s, CH_{2Bim}), 120.7, 127.0, 127.9, 128.2, 128.3, 133.8, 135.4, 137.7 (CH_{Bim} + C_6H_5Sn). Λ_m (DMSO, 10^{-3} M): 32.3 Ω^{-1} cm^2 mol^{-1}. Λ_m (acetone, 10^{-3} M): 0.3 Ω^{-1} cm^2 mol^{-1}.

[Bim($^nBuSnCl_3$)]$_x$ (7). Compound **7** (0.402 g, 0.93 mmol, yield 93%) was prepared following a procedure similar to that reported for **1** using Bim and $^nBuSnCl_3$. Mp 257−260 °C (dec). Anal. Calcd for $C_{11}H_{17}Cl_3N_4Sn$: C, 30.70; H, 3.98; N, 13.02. Found: C, 30.96; H, 3.85; N, 12.89. IR (Nujol, cm^{-1}): 3120w, 3080w, 1572w, 1514m υ(C⋯C, C⋯N), 610br υ(Sn−C), 293s, 284s, 278s υ(Sn−Cl). ^{1}H NMR (DMSO-d_6, 293 K): δ 0.82 (t, 6H, CH_{3Sn}), 1.33 (m, 4H, CH_{2Sn}), 1.63 (m, 8H, CH_{2Sn}), 6.38 (br, 2H, CH_{2Bim}), 7.04 (pd, 2H, CH_{Bim}), 7.49 (pd, 2H, CH_{Bim}), 8.12 (s, 2H, CH_{Bim}). ^{119}Sn NMR (DMSO-d_6, 293 K): −452br, −465. Λ_m (DMSO, 10^{-3} M): 16.9 Ω^{-1} cm^2 mol^{-1}. Λ_m (acetone, 10^{-3} M): 1.2 Ω^{-1} cm^2 mol^{-1}.

[Bim($SnCl_4$)]$_x$ (8). Compound **8** (0.385 g, 0.94 mmol, yield 94%) was prepared following a procedure similar to that reported for **1** using Bim and $SnCl_4$. Mp 250 °C (dec). Anal. Calcd for $C_7H_8Cl_4N_4Sn$: C, 20.57; H, 1.97; N, 13.71. Found: C, 20.74; H, 2.08; N, 13.98. IR (Nujol, cm^{-1}): 3120w, 3110sh, 1522m, 1510m υ(C⋯C, C⋯N), 552br, 380w, 332br, 316br υ(Sn−Cl), 212m. ^{1}H NMR (DMSO-d_6, 293 K): δ 6.63 (s, 2H, CH_{2Bim}), 7.65 (pd, 2H, CH_{Bim}), 7.95 (pd, 2H, CH_{Bim}), 9.29 (s, 2H, CH_{Bim}). ^{1}H NMR (D_2O, 293 K): δ 6.64 (s, 2H, CH_{2Bim}), 7.46 (pd, 2H, CH_{Bim}), 7.66 (pd, 2H, CH_{Bim}), 9.09 (s, 2H, CH_{Bim}). ^{119}Sn NMR (DMSO-d_6, 293 K): −621, −624, −626, −668, −675. Λ_m (DMSO, 10^{-3} M): 21.2 Ω^{-1} cm^2 mol^{-1}. Λ_m (acetone, 10^{-3} M): 1.1 Ω^{-1} cm^2 mol^{-1}.

[Bim($SnBr_4$)]$_x$ (9). Compound **9** (0.500 g, 0.85 mmol, yield 85%) was prepared following a procedure similar to that reported for **1** using Bim and $SnBr_4$. Mp 254 °C (dec). Anal. Calcd for $C_7H_8Br_4N_4Sn$: C, 14.34; H, 1.37; N, 9.55. Found: C, 13.99; H, 1.45; N, 9.37. IR (Nujol, cm^{-1}): 3100w, 1571m, 1533m υ(C⋯C, C⋯N), 549br, 399w, 387w, 320w, 328m, 225m, 211m, 207m υ(Sn−Br). ^{1}H NMR (DMSO-d_6, 293 K): δ 6.67 (s, 2H, CH_{2Bim}), 7.71 (br, 2H, CH_{Bim}), 7.99 (br, 2H, CH_{Bim}), 9.36 (br, 2H, CH_{Bim}). ^{1}H NMR (D_2O, 293 K): δ 6.64 (s, 2H, CH_{2Bim}), 7.46 (pd, 2H, CH_{Bim}), 7.66 (pd, 2H, CH_{Bim}), 9.09 (s, 2H, CH_{Bim}). Λ_m (DMSO, 10^{-3} M): 78.9 Ω^{-1} cm^2 mol^{-1}. Λ_m (acetone, 10^{-3} M): 0.6 Ω^{-1} cm^2 mol^{-1}.

X-ray Powder Diffraction Structural Analysis. The samples were deposited in the hollow of an aluminum holder equipped with a quartz monocrystal zero background plate (except for compound **3** with which a simple aluminum holder was used). Diffraction data (Cu Kα, λ = 1.5418 Å) were collected on a θ:θ vertical scan Bruker AXS D8 diffractometer, equipped with parallel (Soller) slits, a secondary beam curved graphite monochromator, a Na(Tl)I scintillation detector, and pulse height amplifier discrimination. The generator was operated at 40 kV and 40 mA. Slits used: divergence 0.5°, antiscatter 0.5°, and receiving 0.2 mm. Nominal resolution for the present setup is 0.08° 2θ (Mo Kα_1) for the LaB_6 peak at ca. 21.3° (2θ). Other equipment was used for compound **5**: a linear position-sensitive detector (PSD) with a 0.6° divergence slit and receiving 8 mm. All scans were performed in the range 5−105°

Table 1. Crystal Data and Refinement Details for the Compounds **1** and **3**−**6**

	1 Me_2,Cl_2	**3** $^nBu_2,Cl_2$	**4** Ph_2,Cl_2	**5** Me,Cl_3	**6** Ph,Cl_3
empirical formula	$C_9H_{14}Cl_2N_4Sn$	$C_{15}H_{26}Cl_2N_4Sn$	$C_{19}H_{18}Cl_2N_4Sn$	$C_8H_{11}Cl_3N_4Sn$	$C_{13}H_{16}Cl_3N_4Sn$
fw, g mol^{-1}	361.80	452.01	491.98	383.23	450.33
cryst syst	monoclinic	monoclinic	monoclinic	monoclinic	monoclinic
SPGR, Z	$P2_1/n$, 4	$C2/c$, 4	$P2_1/n$, 4	$C2$, 2	$P2/n$, 2
a, Å	15.333(1)	13.182(2)	12.6251(5)	10.706(2)	7.959(1)
b, Å	9.000 (1)	9.903(1)	15.9910(7)	8.217(1)	11.252(1)
c, Å	10.650 (1)	16.349(2)	9.6168(3)	8.077(1)	10.674(1)
β, deg	107.569(3)	98.82(1)	91.496(3)	67.363(4)	111.589(4)
V, Å^3	1401.0(2)	2109.3(4)	1940.9(1)	655.8(2)	888.8(1)
ρ_{calcd}, g cm^{-3}	1.715	1.426	1.684	1.941	1.683
F(000)	696	912	976	366	440
μ(Cu Kα), cm^{-1}	178.8	119.9	130.9	209.6	155.7
diffractometer	Bruker D8	Bruker D8	Bruker D8	Bruker D8	Bruker D8
T, K	298(2)	298(2)	298(2)	298(2)	298(2)
2θ range, deg	5−105	5−105	5−105	5−105	5−105
indexing method	TREOR	SVD	SVD	SVD	SVD
M/GoF	$M(18) = 18$	47.4	65.9	15.04	27.50
N_{data}	5001	5001	5001	5001	5001
N_{obs}	1617	1221	2226	405	1027
R_p, R_{wp}[a]	0.053, 0.153	0.076, 0.178	0.051, 0.084	0.015, 0.095	0.083, 0.120
R_{Bragg}[a]	5.229	10.89	3.374	3.814	3.909
χ^2 [a]	2.888	2.334	1.656	6.108	1.451
V/Z, Å^3	350.2	527.3	485.2	327.9	444.4

[a] $R_p = \sum_i|y_{i,o} - y_{i,c}|/\sum_i|y_{i,o}|$; $R_{wp} = [\sum_i w_i (y_{i,o} - y_{i,c})^2/\sum_i w_i(y_{i,o})^2]^{1/2}$; $R_B = \sum_n|I_{n,o} - I_{n,c}|/\sum_n I_{n,o}$; $\chi^2 = \sum_i w_i (y_{i,o} - y_{i,c})^2/(N_{obs} - N_{par})$, where $y_{i,o}$ and $y_{i,c}$ are the observed and calculated profile intensities, respectively, while $I_{n,o}$ and $I_{n,c}$ the observed and calculated intensities. The summations run over i data points or n independent reflections. Statistical weights w_i are normally taken as $1/y_{i,o}$.

(2θ). Unfortunately, compounds **2** and **7**−**9** showed only a few broad peaks or haloes in their diffraction traces, thus manifesting a nearly amorphous character; even if different synthetic attempts were tried, no (poly)crystalline materials were recovered, and therefore, their structural properties remain unknown.

Standard peak search methods and indexing of the first lines (2θ < 30°) by TOPAS-R and TOPAS-I (Bruker AXS, 2005) allowed determination of the lattice parameters (see Table 1) for all compounds **3**−**6**. Successful Le Bail refinement confirmed the absence of spurious peak; systematic absences, density, and geometrical considerations indicated space groups $C2/c$, $P2_1/n$, $C2$, and $P2/n$ for **3**, **4**, **5**, and **6**, respectively. Successful structure solutions and refinements confirmed these cell and space group choices.

A special comment requires the correct space-group determination of compound **1**. Indeed, similar agreement factors (in the 14−17% range for data up to 2θ = 55°) were obtained using, in a Le Bail simulation, a number of possible space groups where at most *one* very minor (but variable) peak was not fit if systematically absent classes were introduced. Taking into account that a contaminant phase can always be present in an analytically pure bulk material, body-centered and primitive lattices sharing a number of symmetry operations were initially considered probable. Density considerations clearly indicated that the proposed unit cell, obtained by the indexing process described above, contains four formula units, i.e., $Z = 4$. Helping the correct assignment, we resorted to solid-state ^{13}C CP-MAS NMR measurements, which clearly indicated the presence of seven distinct peaks attributable to the Bim ligand (at δ = 116.4, 119.0, 127.0, 130.2, 139.7, and 141.9 ppm for the ring CH moieties and δ = 59.4 ppm for the methylene bridge), thus imposing a $Z' = 1$ value. Consequently, for the $SnCl_2Me_2$ moiety, to which Bim is bound, one crystallographically independent or two-half moieties lying about a symmetry element can be expected. No matter which model is adopted, the presence of a single CH_3 peak at δ = 27.2 ppm speaks for an occasional coincidence of the methyl peaks. With these observations in mind we could exclude a number of space groups (particularly the primitive acentric ones, requiring doubling of the Bim moieties) and forced by the presence of weak, but non-negligible, *indexed* peaks, we eventually solved and refined the whole model in $P2_1/n$ (with two Sn(IV) atoms in *I-related* inversion centers, thus explaining the difficulty in determining the correct lattice symmetry). The most evident chemical consequence of this choice is the *trans*-$SnCl_2Me_2$ geometry of both crystallographically independent metal fragments and exclusion, from NMR data, of local disorder by mutual exchange of the nearly isosteric chloride and methyl residues. As further spectroscopic information two satellites surround the CH_3 peak, attributed to the heteronuclear coupling, ^1J(C−Sn), of about 580 Hz.

The structural models employed in the final whole-pattern Rietveld-like refinement were determined ab initio by the simulated annealing technique implemented in TOPAS-R using a 'flexible' rigid body for the Bim ligand (the free conformational parameters were the torsional angles about the two N−CH_2 bonds). A few restraints were added to obtain chemically significant geometrical values. In a few cases a preferred orientation correction was applied (only if strictly necessary). Table 1 contains the relevant crystallographic data and structure refinement details. The final Rietveld refinements plots are included in the Supporting Information.

Thermodiffractometric Analysis and Evaluation of the Thermal Strain Tensors. Thermodiffractometric experiments were performed in air from 25 to ca. 300 °C using a custom-made sample heater, assembled by Officina Elettrotecnica di Tenno, Ponte Arche, Italy. Diffractograms at different temperatures (with steps of 20 °C) were recorded typically in the range 5−30° 2θ. Linear, parametric Le Bail refinements, as described in ref 21, eventually afforded the 'best' set of cell parameters at the different temperatures. Linear thermal expansion coefficients were then derived from $(1/x)(\partial x/\partial T)$ vs T plots (x being either a lattice parameter or the cell volume). Later, for each compound we selected the cell data at two well-separated temperatures (typically RT and the last useful point before decomposition) and computed the thermal strain tensor and its eigenvalues and eigenvectors using a locally developed

(21) Stinton, G. W.; Evans, J. S. O. *J. Appl. Crystalllogr.* **2007**, *40*, 87−95.

program based on the Ohashi algorithm.[22] Thermal strain tensors were visualized with WinTensor,[23] which produces a VRML[24] three-dimensional surface to be displayed together with the (properly oriented) whole crystal structure[25] with the CORTONA VRML client.

Results and Discussion

Synthesis and Spectroscopy. The reaction of Bim with R_nSnX_{4-n} acceptors in alcohols or diethyl ether or alcoholic: diethyl ether mixtures yielded adducts **1**−**9** always as insoluble colorless precipitates. All derivatives are poorly soluble in methanol and soluble or moderately soluble in DMSO. Derivatives **8** and **9**, poorly soluble in DMSO, are soluble in water. Broadly speaking, yields are generally very high in solvents such as diethyl ether, ethanol, and ethanol/diethyl ether mixtures, whereas they appear somewhat lower in "coordinating" solvents such as acetone or acetonitrile, promoting chain termination. Various amounts of water are present in the original precipitates, likely due to trace amounts of moisture in the starting reagents that can be removed by heating the precipitate to 80 °C. It is worth noting that the tetra- and trihalotin(IV) derivatives are afforded in high yield immediately upon mixing a solution of Bim and R_nSnX_{4-n}, whereas formation of the dihalotin species requires longer reaction times and nonionizing solvents. Yields of the reactions are strongly dependent on the nature and quantity of the solvents employed. The ligand Bim could be employed for the selective extraction of $RSnX_3$ with respect to R_2SnX_2: if an ethanol solution containing 1 mmol of Bim was added to an ethanol solution containing 1 mmol of both Me_2SnCl_2 and $MeSnCl_3$, [Bim($MeSnCl_3$)] exclusively formed, Me_2SnCl_2 being completely recovered from the solution.

The IR spectra of the ligand Bim and its derivatives exhibit weak vibrations at ca. 3000 cm^{-1} due to CH stretching of the heterocyclic rings and other intense absorptions between 1700 and 1500 cm^{-1} typical of ring breathing.[26] In the far-IR region the spectra of compounds **1**−**9** are similar to those reported for bis(pyrazol-1-yl)alkane derivatives.[27] The strong absorption at ca. 570 cm^{-1} found in the dimethyltin(IV), assigned to ν_{asym} Sn−C, is consistent with a *trans*-R_2Sn configuration.[28] The ν_{asym} Sn−C in the diphenyltin complex is found at ca. 290 cm^{-1}, always suggesting a *trans*-Ph_2Sn geometry.[29] The $RSnX_3$ adducts show, as expected, a single Sn−C vibration at around 270 (R = Ph), 540 (R = Me), and 610 (R = Bu^n) cm^{-1}. In addition, in the phenyltin(V) derivatives two weak absorptions in the 170−300 cm^{-1} region and other more intense bands at ca. 450 cm^{-1} can always be detected. These bands can be assigned to "in-plane phenyl ring rotation" (Whiffen's u notation), "out-of-plane phenyl ring bending" (x), and "out-of-plane bending" (y).[30] At variance, the tin−halogen stretching frequencies may be assigned with more certainty. In the diorganotin species these bands occur at ca. 260 cm^{-1}. In the tri- and tetrahalide adducts the same absorptions fall in the 300−270 and 330−300 cm^{-1} region, respectively, shifted to lower frequency with respect to the same absorptions in the parent R_nSnX_{4-n} and close to those reported for phenanthroline and bipyridyl adducts.[31]

The ^{1}H NMR spectra in alcohols, water, or when not possible in DMSO-d_6 always support the formulas proposed and show that Bim has not undergone any structural change upon coordination. The spectra indicate that the diorganotin complexes completely dissociate in DMSO-d_6, their proton chemical shifts being analogous to those found in the same solvents for the free Bim ligand, giving further support for the occurrence of reaction assessed from both conductivity and MW determinations. On the other hand, a not-negligible downfield shift is always found in the tri- and tetrahalide derivatives, which suggests persistence of the coordination of Bim to the tin moiety in solution, likely upon breaking only one of the bridging Sn−N(imidazolyl) bonds and formation of dimers, oligomers, or mononuclear species such as those reported in the drawing. This hypothesis is supported by both ^{119}Sn NMR spectra of compounds **5** and **7**−**8**, which exhibit signals analogous to that found in complexes of formula $RSnCl_3(N_2$-donor) (R = Me, Bu, or Cl), and the $^1J(^1H-^{119}Sn)$ coupling constant calculated for **5**, which is of the same order of magnitude as $MeSnCl_3(N_2$-donor) previously reported.[32]

Crystal Chemistry. Crystals **1** and **3**−**6** share the presence of polymeric one-dimensional, 'linear' (all the metals in a chain belong to a straight line), −Bim−Sn−Bim− chains, based on Sn(IV) octahedral metal centers. These chains are invariably isooriented, i.e., parallel packed; however, the presence of different ancillary ligands completing the octahedral Sn coordination somewhat modulates their 2D organization in the orthogonal plane (see below for details and a correlation between the thermodiffractometric behavior and chain organization). Further modulation factors are the stereochemistry of the N−Sn−N linkage, which is trans in all derivatives but in **4**, and the conformation of the Bim ligand, which has idealized C_2 symmetry in all derivatives but in **4** where the idealized symmetry is C_s (see below and Figure 1 for a discussion of Bim stereochemistry in terms of the two torsional angles, τ_1 and τ_2, defined in Chart 1).

Crystal Structures of 1 and 5. These two compounds, [Bim(Me_2SnCl_2)]$_n$ and [Bim($MeSnCl_3$)]$_n$, respectively, differ only in the substitution of a methyl with a nearly isosteric chloride ligand, and we expect a substantial similarity of their

(22) Ohashi, Y. In *Comparative Crystal Chemistry*; Hazen, R. M., Finger, L. W., Eds.; Wiley: New York, 1982; pp 92−102.
(23) WinTensor, coded by W. Kaminsky, Department Of Chemistry, University Of Washington; 2004.
(24) Virtual Reality Mark-up Language.
(25) Crystal structures VRML pictures produced with WebLab ViewerLite 3.5.
(26) Nieuwport, G.; Vos, J. G.; Groeneveld, W. L. *Inorg. Chim. Acta* **1978**, *29*, 117−123.
(27) Pettinari, C.; Lorenzotti, A.; Sclavi, G.; Cingolani, A.; Rivarola, E.; Colapietro, M.; Cassetta, A. *J. Organomet. Chem.* **1995**, *496*, 69−85.
(28) Clark, J. P.; Wilkins, C. J. *J. Chem. Soc. A* **1966**, 871−873.
(29) May, R. J.; McWhinnie, W. R.; Poller, R. C. *Spectrochim. Acta* **1971**, *27A*, 969. Smith, A. L. *Spectrochim. Acta* **1968**, *24A*, 695−706.
(30) Dance, M. C.; McWhinnie, W. R.; Poller, R. C. *J. Chem. Soc., Dalton Trans.* **1976**, 2349−2350.
(31) Visalakshi, R.; Jain, V. K.; Kulshreshtha, S. K.; Rao, G. S. *Inorg. Chim. Acta* **1986**, *118*, 119−124.
(32) Pettinari, C.; Marchetti, F.; Cingolani, A.; Bartolini, S. *Polyhedron* **1996**, *15*, 1263−1276.

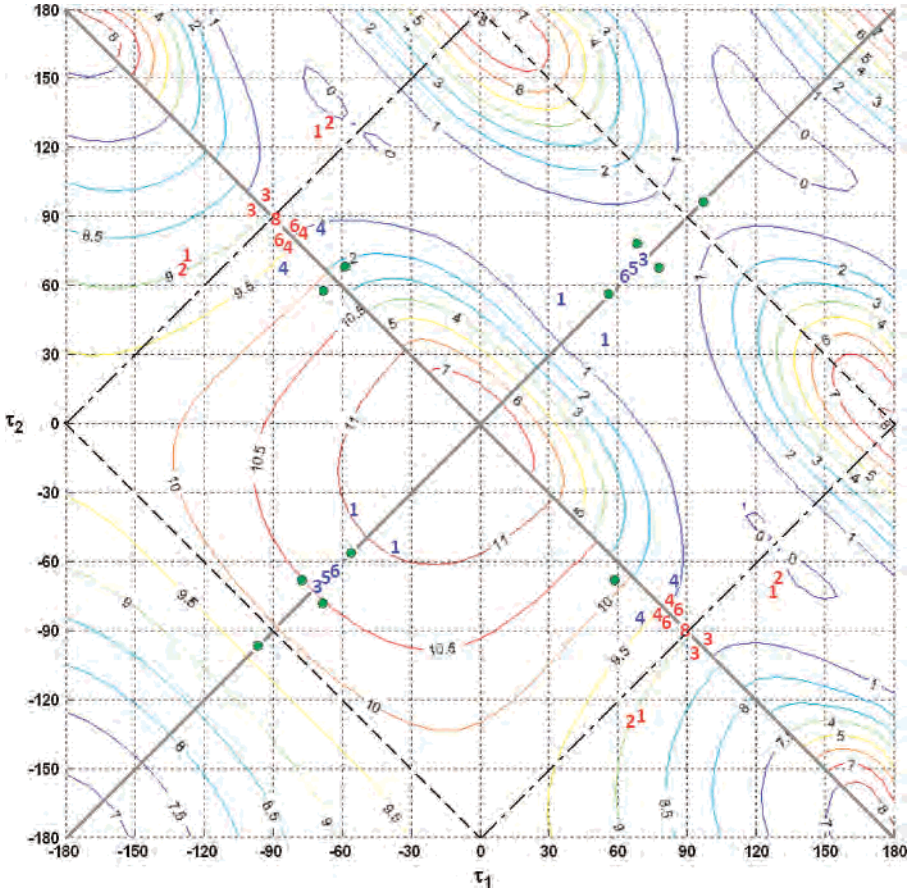

Figure 1. "Ramachandran plots" obtained by systematic variations of Bim conformation (for a definition of τ_1 and τ_2, see Chart 1). (Upper triangle) Potential-energy surface of the 'free' Bim ligand (computed using Tinker and the MM3 force field). (Lower triangle) Expected M···M distance computed for a flexible M−BIM−M fragment with standard C−C, C−N, and M−N (2.40 Å) bond lengths. Blue and red numbers address the compounds described in the present and following pares, respectively. Green circles concern Btm derivatives which will be the subject of a forthcoming publication. All experimental observations have been replicated according to the symmetry of the potential-energy surface of the free ligand [(τ_1, τ_2), ($-\tau_1$, $-\tau_2$), (τ_2, τ_1), ($-\tau_2$, $-\tau_1$)]. Continuous ($\tau_1 = \tau_2$ and $\tau_1 = -\tau_2$), dashed, and dot−dashed lines highlight C_2, C_s, pseudo-C_s, and pseudo-C_2 conformations, respectively.

Table 2. Synoptic Collection of Relevant Structural and Stereochemical Features of Compounds **1** and **3**−**6**

	1	**3**	**4**	**5**	**6**
topology	1D	1D	1D	1D	1D
geometry	octahedral	octahedral	octahedral	octahedral	octahedral
coordination	$N_2C_2Cl_2$	$N_2C_2Cl_2$	$N_2C_2Cl_2$	N_2CCl_3	N_2CCl_3
M−N, Å	2.31, 2.32	2.17(×2)	2.46, 2.54	2.29(×2)	2.31(×2)
M−Cl, Å	2.43, 2.45	2.33(×2)	2.56, 2.60	2.28,[a] 2.49(×2)	2.37(×2), 2.55
M−C, Å	2.12, 2.20	2.12(×2)	2.12, 2.14	2.29[a]	2.08
M−bim−M, Å	11.09	9.68	9.62	10.64	10.67
N−Sn−N, deg	180	180	92.1	173.4	174.6
τ_1, deg	38.8	70.7	-69.4	67.6	64.7
τ_2, deg	52.2	70.7	84.4	67.6	64.7
idealized Bim symmetry	C_2	C_2	C_s	C_2	C_2
M site symmetry	−1	−1	1	2	2

[a] These anomalous values arise from Me/Cl disorder (refined occupancies 0.41(4):0.59(4)).

crystal structures; however, this does not occur. Certainly **1** and **5** share a similar C-centered rectangular chain packing (in **1** nearly hexagonal); however, as shown in Figure 2, their polymeric backbones have a different arrangement. Indeed, they differ both in the local Sn stereochemistry (the trans Bim ligands being eclipsed within themselves and to the chlorine atoms in **1** while substantially staggered in **5**) and in the relationships between nearby metals: in **1** the chain is generated by two independent (half) tin atoms which are mutually eclipsed but alternate methyl and chlorine ligands, while in **5** all metals are crystallographically equivalent and no ligand alternation is observed. As addressed in Table 2, the chlorine and carbon atoms on the two-fold axis are mutually disordered.

Crystal Structure of 3. $[Bim(^nBu_2SnCl_2)]_n$ chains (of marked ellipsoidal shape) share with **1** and **5** a C-centered rectangular packing; this is somewhat unusual since we would expect the ^{n}Bu ligands of different chains to intermingle rather than be buried within each individual chain in the 'holes' created by the Bim ligand as shown in Figure 3.

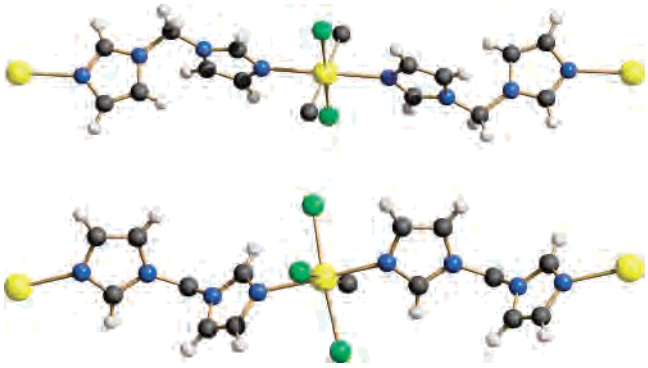

Figure 2. Schematic drawing of the portion of the one-dimensional chain present in $[Bim(Me_2SnCl_2)]_n$ (**1**; top) and $[Bim(MeSnCl_3)]_n$ (**5**; bottom). The polymers grow along [1 0 2] and [−1 0 1], respectively. Tin atoms are shown in yellow and chlorine atoms in green.

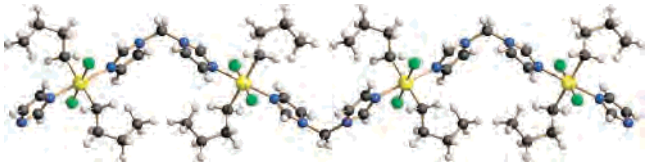

Figure 3. Schematic drawing of the portion of the one-dimensional chain present in $[Bim(^nBu_2SnCl_2)]_n$ (**3**). The polymer grows along [1 0 1]. Tin atoms are shown in yellow and chlorine atoms in green.

As far as the stereochemistry of the Sn atom is concerned, we notice that the two trans Bim ligands are eclipsed within themselves and to the chlorine atoms (like in **1**).

Crystal Structures of 4 and 6. These two compounds, $[Bim(Ph_2SnCl_2)]_n$ and $[Bim(PhSnCl_3)]_n$, share similarities in the packing since in both cases the phenyl substituents protrude from the backbone and intermingle with those of the nearby chains. However, in **4** these interlocking phenyls are mutually orthogonal, while in **6** they are mutually parallel and 'segregated'. Indeed, when the structure of **6** is viewed along the chain axis (*c*) as in Figure 4 it is possible to recognize that chain backbones are organized as double layers separated by layers of stacked phenyls which allow for some narrow channels among them (radius 1.40 Å, volume 118 Å^3). At variance, no empty volume is left in the packing of **4**. Species **4** and **6**, as shown in Figure 5, differ even more in their polymeric backbones since in **4** there are cis N−Sn−N linkages and Bims with C_s conformations while in **6** there are trans linkages and C_2 Bims. As shown in the following paper, cis N−Sn−N linkages and C_s Bims are not unusual; moreover, **4** is isostructural to $(Btm)SnPh_2Br_2$ (Btm = bis(triazolyl)methane).[33]

Isobaric Thermal-Expansion Coefficients and Strain Tensors. To attempt a correlation between RT structures and anisotropy of intermolecular forces we determined, for all compounds structurally characterized here, the thermal behavior of their lattice parameters between RT and their decomposition/melting temperature (see Figure 6 for the relative variations with temperature of the cell axis). This allowed us to compute their thermal-expansion coefficients (Table 3) and thermal strain tensors (Table 4). Strain tensors

(33) To which **4** it is almost isomorphous: Tang, L.-F.; Wang, Z.-H.; Chai, J.-F.; Jia, W.-L.; Xu, Y.-M.; Wang, J.-T. *Polyhedron* **2000**, *19*, 1949−1954.

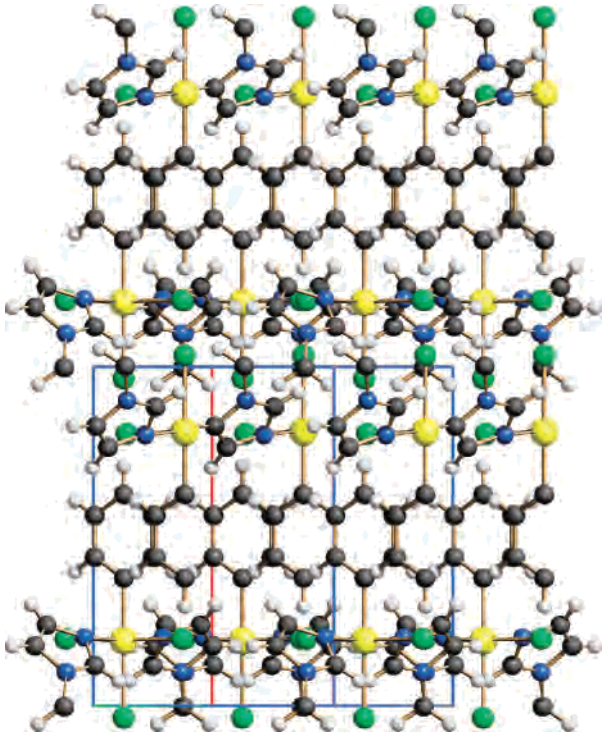

Figure 4. Crystal packing of $[Bim(PhSnCl_3)]_n$ (**6**) down [0 0 1] highlighting the double layers (stacked along *b*) described in the text. Tin atoms are shown in yellow and chlorine atoms in green.

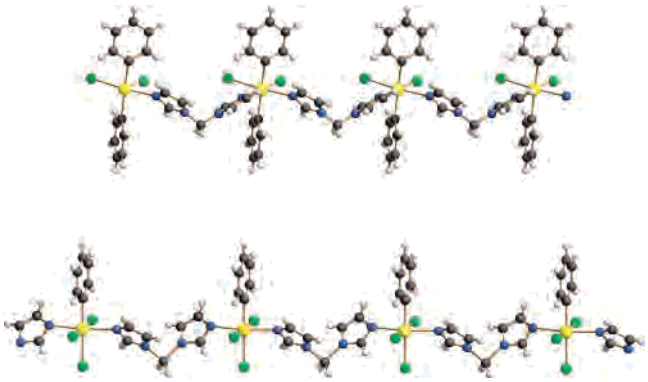

Figure 5. Schematic drawing of the portion of the one-dimensional chain present in $[Bim(Ph_2SnCl_2)]_n$ (**4**; top) and $[Bim(PhSnCl_3)]_n$ (**6**; bottom). Both polymers grow along [0 0 1]. Tin atoms are shown in yellow and chlorine atoms in green.

are particularly useful, because, when drawn within the structure packing diagrams (see Figures 7 and 8), they convey information otherwise inaccessible. This is particularly true for low-symmetry (monoclinic and triclinic) crystal systems where thermal expansion coefficients, being somewhat 'correlated' by the variations of the interaxial angles, may conceal some significant structural effect.

Thermal expansion depends on the strengths of chemical 'interactions' in different directions. Actually, deformation of a crystal by a change in the temperature is expected to be minimal in the direction of the highest atomic density, i.e., the direction of strongest interactions. Therefore, the principal axes of the thermal strain tensor, being directed toward the softest and hardest expansion directions, should straightforwardly highlight weak and strong 'intermolecular' interactions. Polymers are long molecules with 'strong' covalent

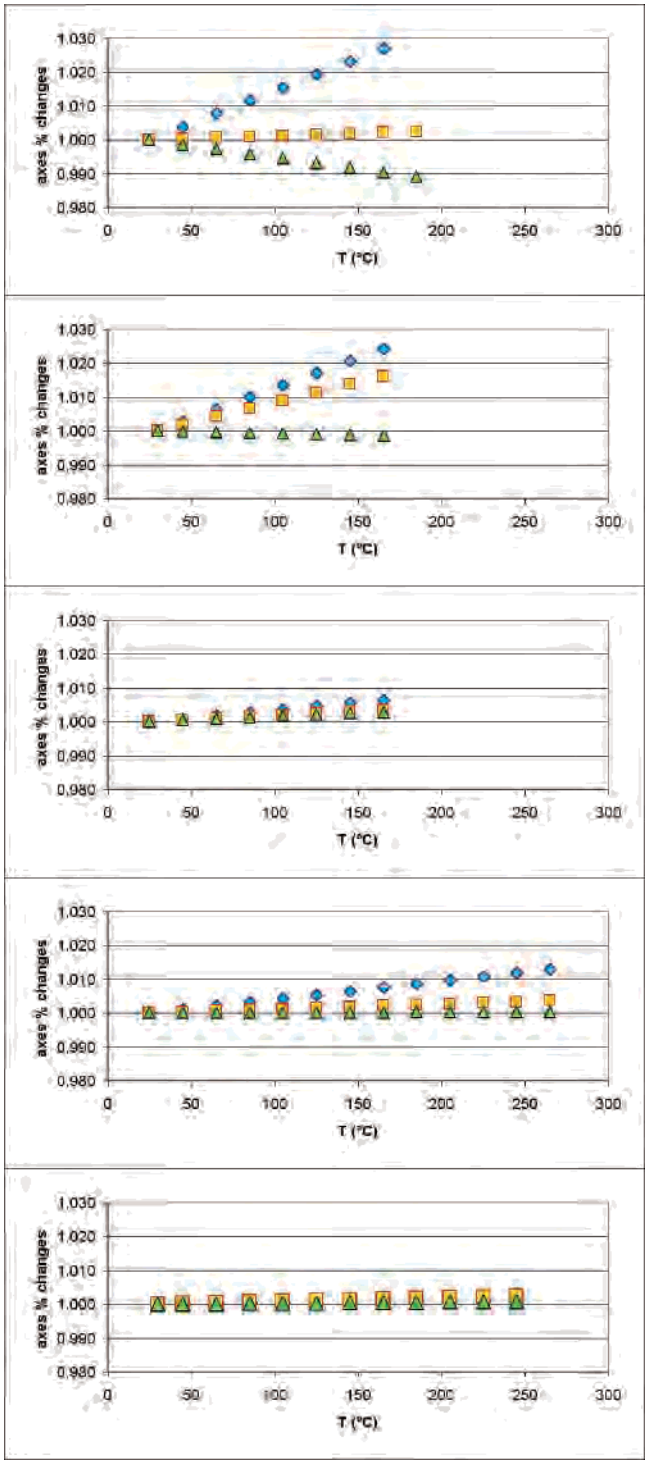

Figure 6. Plots of the relative variations of the cell axes vs temperature for compounds **1**, **3**, **4**, **5**, and **6** (top to bottom): (■) *a* axis, (♦) *b* axis, and (▲) *c* axis.

bonds in the chain direction and 'weak' intermolecular forces holding together adjacent chains in perpendicular directions. A large anisotropy is therefore expected. Moreover, since thermal agitation gives rise to lateral vibrations in the chain, an effective contraction may also be observed.

Indeed, all compounds but **4** have a negative strain component (cf. values in Table 2 and 4). This complicates the above picture since now the smallest (positive) strain is no longer isooriented with the chains. Actually, chains

Table 3. Thermal Expansion Coefficients for Compounds **1** and **3**−**6**[a]

compound	α_a[b]	α_b	α_c	α_V
1	1.50	19.37	−6.86	15.92
3	11.90	18.07	−1.01	29.09
4	4.61	2.50	2.06	9.22
5	1.47	5.40	−0.09	6.77
6	0.54	1.12	0.33	3.09

[a] The quoted values are taken as the average linear expansivities. [b] α_x is defined as $(1/x)(\partial x/\partial T)$ in units of 10^{-5} °C^{-1}.

invariably 'bisect' these two strain components; that is, they point toward an almost 'zero strain' direction (which however is not one of the principal axis of the strain tensor, see Figure 7). On the contrary, in the absence of a negative strain component, like in **4**, the 'rigid' polymeric backbone is, as expected, isooriented with the smallest strain component (see Table 4).

Figure 3 and Tables 3 and 4 offer a comparative view of the thermal behavior of the five crystalline samples analyzed here. What is clear at a first sight is that **1** and **3** and, to a lesser extent, **5** undergo significant changes under thermal stress; at variance, **4** and **6** are only marginally perturbed. It seems obvious to correlate this different behavior with the absence (in **1**, **4**, and **5**) or presence (in **4** and **6**) of ligand entanglement of nearby polymeric chain as discussed above. Although to a much lesser extent, because of phenyl entanglement, **6** also shows some thermal expansion which, highly anisotropic in nature, clearly highlights that the softer direction matches the sliding of the phenyl groups one on top of the other (see Figure 8).

The thermal strain tensors of **3**−**5** isooriented with their crystal packings are reported as Supporting Information.

Conformational Analysis of the BIM Ligand. In order to quantitatively address the stereochemistry of Bim, we found it useful to employ two torsional angles, τ_1 and τ_2, defined by the $C_N-N-C_{H2}-N$ sequence, i.e., those involving the orientation of each of the imidazole rings with respect to the N-methylene bridge (see Chart 1) and compute (using Tinker[34] program and the MM3[35] force field therein tabulated) the Ramachandran plot of Figure 1 (upper triangle), which highlights the conformational preferences of the free Bim ligand. In the lower triangle of Figure 1 are instead reported the M···M distances spanned by Bim as a function of the very same degrees of freedom computed for a flexible M−Bim−M fragment with standard C−C, C−N, and M−N (2.40 Å) bond lengths. On the whole, the pseudo-Ramachandran plot of Figure 1 highlights the spectrum of 'possible' (i.e., associated to a low energy conformation of the free ligand) M···M distances.

Note that with this choice $\tau_1 = \tau_2$ means rigorous C_2 symmetry while $\tau_1 = -\tau_2$, defines the C_s one. We can also consider pseudo-C_2 ($\tau_1 = \tau_2 \pm 180$) and pseudo-C_s ($\tau_1 = -\tau_2 \pm 180$) conformations which share similar steric energies with their C_2 and C_s counterparts: the rotation of 180° about the $N-C_{H2}$ bond interchanging N with the nearby CH do

(34) Ponder, J. W.; Richards, F. M. *J. Comput. Chem.* **1987**, *8*, 1016−1024.
(35) Allinger, N. L.; Yuh, Y. H.; Lii, J.-H. *J. Am. Chem. Soc.* **1989**, *111*, 8551−8566.

Table 4. Strain Tensors Principal Axes (Lengths and Orientations) for Compounds **1** and **3**−**6**

	chain direction	ΔT	$\alpha 1^a$	u^b	v^b	w^b	$\alpha 2^a$	u^b	v^b	w^b	$\alpha 3^a$	u^b	v^b	w^b
1	(1 0 2)	160	−1.16	−0.14	0	1	0.62	2.92	0	2	3.10	0	1	0
3	(1 0 1)	140	−0.15	0.13	0	1	1.61	−1	0	−0.04	2.44	0	−1	0
4	(0 0 1)	140	0.29	−0.03	0	1	0.35	0	−1	0	0.64	1	0	0.09
5	(−1 0 1)	240	−0.03	−1	0	3.85	0.35	1	0	−0.06	1.30	0	1	0
6	(0 0 1)	220	−0.10	−1.18	0	1	0.25	0	1	0	0.54	1.42	0	1

[a] Strain, change in length per unit length, is dimensionless (all values multiplied × 10^2). For a better comparison with the data in Table 2 we also report the pertinent ΔT values. [b] ***u***, ***v***, ***w*** are the (fractional) Miller indexes of the given principal axis direction.

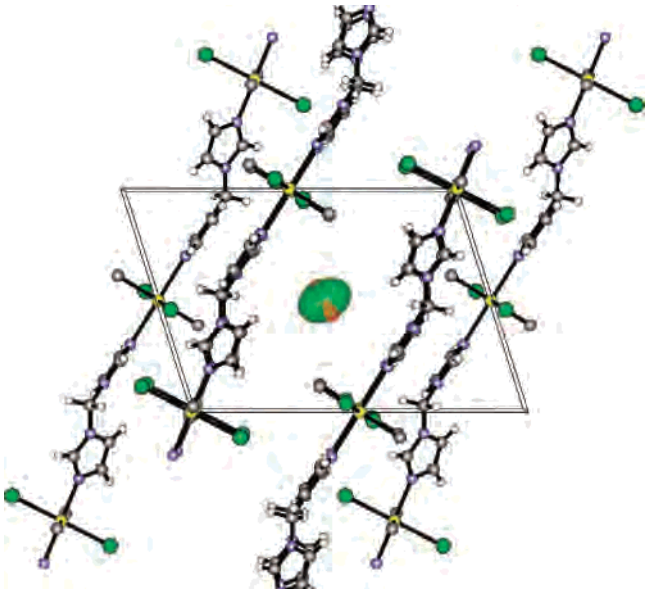

Figure 7. Thermal strain tensor of $[Bim(Me_2SnCl_2)]_n$, **1**, isooriented with its crystal packing, viewed down the largest strain component [010]. Horizontal axis: *a*. Green portions indicate expansion, while the red one highlights (minor) contraction directions (approximately aligned with *c*). Note that chains 'bisect' the two smallest (one positive, one negative) strain components pointing toward an almost 'zero-strain' direction (which however is not one of the principal axes of the strain tensor).

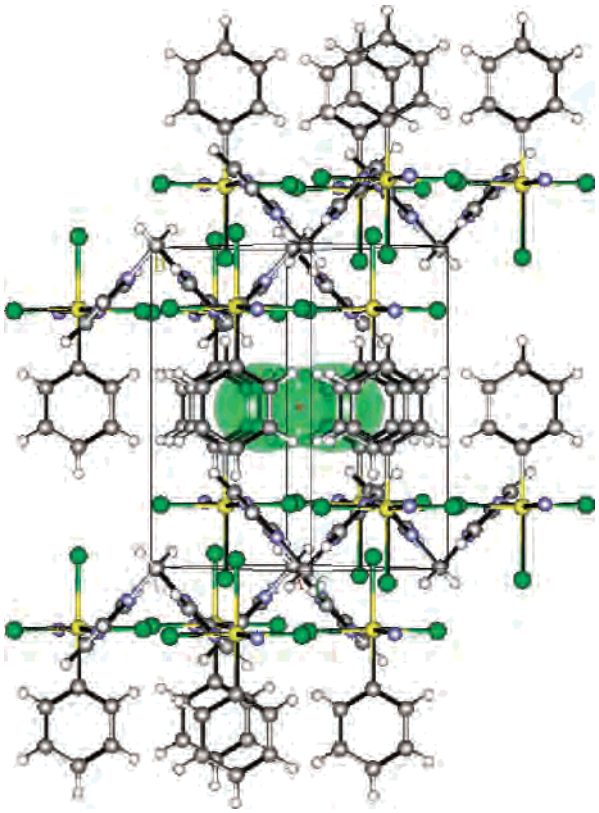

Figure 8. Thermal strain tensor of $[Bim(PhSnCl_3)]_n$, **6**, isooriented with its crystal packing, viewed down the negative strain component [−101]. Vertical axis: *b*. The softest direction matches the sliding of the phenyl groups one on top of each other. Note that strain tensors in these figures are shown with arbitrary scale in order to highlight their directionality and anisotropy. Therefore, that in Figure 7 appears much smaller, but as indicated by the numbers collected in Table 4, its absolute values are much larger.

not substantially modify the steric energy. C_2 and pseudo-C_s conformations are inherently *E* (binding metals on opposite sides of the Bim root-mean-square plane) at variance C_s and pseudo-C_2 conformations are inherently *Z*.

Markers in Figure 1 address the experimental Bim conformations found in the compounds described in the present and following article. They clearly cluster in regions with a relative steric energy smaller than 3 kcal mol^{-1}. Assuming this value as a threshold, it is clear that C_2 (and pseudo-C_2) conformations can be easily deformed, retaining their symmetry, but this is not true for C_s (and pseudo-C_s) conformations whose field of existence is much narrower. Moreover, by comparing the lower and upper triangles of the Ramachandran plot of Figure 1 it is clear that C_2 conformations span a wide range of possible M···M contacts (roughly between 7.5 and 11 Å) while the C_s ones are restricted to a narrower range (8.5 − 10 Å). At variance, the energy range spanned by the experimental C_s conformations seem to be slightly larger than that spanned by the C_2 ones; this could imply than C_s conformations 'exist' in slightly more crowded environments than the C_2 ones. In fact, all C_s conformations found in this and the following paper are associated with smaller N−M−N angles (90−118.5°) than the C_2 ones (173.4−180°).

Finally, $\tau_1 = -\tau_2 \pm 90$ addresses a low-energy region of the potential-energy surface associated to disrotation of the two imidazole rings, which, however, has not yet been found to be populated for coordinated Bim apart from, at the intercepts, the more (experimentally) populated C_2 and pseudo-C_2 regions.

Conclusions

New polynuclear coordination species containing the ditopic bis(1-imidazolyl)methane ligand have been prepared as microcrystalline powders by reacting Bim with R_nSnX_{4-n} acceptors in alcohols, diethyl ether, or alcoholic:diethyl ether mixtures. The derived adducts of ligand-to-metal 1:1 ratio have been characterized by analytical and spectroscopic methods as well as, above all, less conventional powder diffraction techniques. The crystal and molecular structures

derived there from unambiguously showed that all consist of 1D chains with octahedral tin atoms with trans N−Sn−N linkages (except **4**, which displays a cis N−Sn−N linkage).

The Bim ligand, which possesses two torsional degrees of freedom (about the two CH_2−N bonds), was found to preferentially adopt a (idealized) C_2-symmetric conformation, although in **4** Bim has an idealized C_s symmetry. Whether this is related to the trans vs cis arrangement of the N−M−N angles is difficult to demonstrate, even if easy to observe. However, insight on the stereochemical preferences of the Bim ligand has been obtained by constructing and analyzing the Ramachandran plot of Figure 1.

Finally, all systems described here have also been characterized by thermodiffractometry, monitoring the evolution of the lattice parameters on varying the temperature. From these measurements we derived thermal expansion coefficients and strain tensors which we used to interpret thermally induced transformations (and, tentatively, the dynamics of the chains in these soft lattices) on the light of the RT crystal structures.

Acknowledgment. This work was supported by the Italian MUR (PRIN2006: "Materiali Ibridi Metallo-Organici Multifunzionali con Leganti Poliazotati"). The Fondazione Provinciale Comasca is acknowledged for partial funding. We thank Dr. Simona Galli (University of Insubria) for helpful discussions.

Supporting Information Available: Crystallographic data (excluding structure factors) for the structures reported in this paper have been deposited with the Cambridge Crystallographic Data Center as supplementary publication no. CCDC 655208−655212. Copies of the data can be obtained free of charge on application to the Director, CCDC, 12 Union Road, Cambridge, CB2 1EZ, UK (Fax: +44−1223-335033; e-mail: deposit@ccdc.cam.ac.uk or http://www.ccdc.cam.ac.uk).

IC701530C